Journal of Alloys and Compounds 505 (2010) 157–162

Contents lists available at ScienceDirect

Journal of Alloys and Compounds

journal homepage: www.elsevier.com/locate/jallcom

Zirconium–indium intermetallic compounds investigated by measurements of nuclear electric quadrupole interactions

H. Saitovitch, P.R.J. Silva, J.T. Cavalcante, M. Forker*

Centro Brasileiro de Pesquisas Físicas, Rua Dr. Xavier Sigaud 150, Rio de Janeiro, RJ, CEP 22290-180, Brazil

ARTICLE INFO

Article history:
Received 30 April 2010
Received in revised form 30 May 2010
Accepted 1 June 2010
Available online 11 June 2010

PACS:
76.80.+y
75.20.En

Keywords:
Zr–In intermetallic compounds
Nuclear electric quadrupole interactions
Perturbed angular correlations

ABSTRACT

The nuclear electric quadrupole interaction (QI) of the nuclear probe ^{111}Cd on In sites of intermetallic compounds of the Zr–In system has been investigated as a function of temperature ($15 \leq T \leq 1200$ K) by perturbed angular correlation (PAC) spectroscopy. Zr–In compounds were synthesized by arc-melting of the metallic constituents and doped with ^{111}In, the mother isotope of the probe nucleus by diffusion at 1200 K. Strength, symmetry and temperature coefficient of the electric field gradient (EFG) were determined for four In sites: the two 8*e*-sites of $ZrIn_2$ and sites (2*b*, 4*d*) of β-$ZrIn_3$. The temperature dependence of the relative intensities of these sites in the PAC spectra provides information on Zr–In solid state reactions occurring during annealing of arc-molten Zr–In ingots.

1. Introduction

The experimental information available on the five intermetallic phases of the zirconium–indium system [1] is rather limited. The structures and lattice parameters of $ZrIn_3$ (tetragonal Al_3Zr-type structure at low, Al_3Ti-type structure at high temperatures), $ZrIn_2$ (tetragonal $HfGa_2$-type), ZrIn (cubic Cu-type), Zr_2In (cubic AuCu-type), and Zr_3In (cubic $AuCu_3$-type) have been established decades ago (Refs. [2–4]). Since then, only $ZrIn_2$ has received somewhat more attention. Meschel and Kleppa [5] have determined the standard enthalpy of formation of $ZrIn_2$. Zumdick et al. [6] have extracted structure details of $ZrIn_2$ from single-crystal X-ray diffraction data and investigated the charge distribution and chemical bonding by electronic structure calculations. Zr_2In is mentioned in a study of the interaction between the components of the Zr–Mn–In system by Gulay and Zaremba [7]. The information on the Hf–In phase diagram is even scarcer [8]. Only Hf_2In_5 [4,9] has been studied in some detail. For the Hf–In phase $HfIn_2$ a AuCu-type superstructure has been suggested [8].

In this communication we report an investigation of Zr–In intermetallic phases by measurements of electric quadrupole interactions (QI) between the quadrupole moment of a probe nucleus and the electric field gradient (EFG) at the probe site. The EFG reflects the charge distribution surrounding the probe nucleus. Measurements of QI's may therefore provide information on the structural and electronic properties of the host material.

The present study was carried out with the perturbed angular correlation (PAC) technique. Among the numerous radioisotopes suitable for PAC studies, ^{111}Cd and ^{181}Ta offer the most favourable overall conditions and therefore take leading positions in statistics on PAC measurements. The excited states of ^{111}Cd are populated in the EC decay of ^{111}In ($T_{1/2} = 2.8$ d), those of ^{181}Ta in the β^- decay of ^{181}Hf ($T_{1/2} = 42$ d). The recoil involved in these decays is too small to dislocate the daughter isotopes from their lattice position. It is therefore safe to assume that in Zr–In compounds the PAC probe ^{111}Cd resides on substitutional In sites. Because of the pronounced chemical similarity of Hf and Zr, it can be presumed that ^{181}Ta substitutes Zr in Zr–In compound. In spite of this attractive situation of two different PAC probes on *a priori* known sites of the same compound, Zr(Hf)–In phases are not found among the many ^{111}Cd and ^{181}Ta PAC studies of intermetallic compounds.

One of the advantages of PAC when compared to other hyperfine spectroscopic techniques results from the fact that this method does not depend – as NMR/NQR or nuclear orientation – on the population differences of the hyperfine levels nor – as Mössbauer spectroscopy – on the Debye–Waller factor of the investigated compound. Therefore the sensitivity of PAC spectroscopy to hyperfine interaction is temperature independent and its temperature

* Corresponding author. Tel.: +55 21 2141 7157; fax: +55 21 2141 7330.
E-mail address: forker@hiskp.uni-bonn.de (M. Forker).

0925-8388/$ – see front matter © 2010 Elsevier B.V. All rights reserved.
doi:10.1016/j.jallcom.2010.06.018

range in principle unlimited. This makes PAC a powerful tool when material properties at high temperatures are to be investigated by measurements of hyperfine interactions. PAC measurements up to $T \sim 2350$ K have been reported [10]. Recent examples of high-temperature PAC studies of intermetallic compounds include the investigation of tracer diffusion [11], of solute site preference [12] and solute EFG's [13] up to temperatures $T \sim 1200$ K.

Here we present a PAC investigation of the QI of ^{111}Cd in several Zr–In phases in the temperature range $15 \leq T \leq 1200$ K. A similar study with the PAC probe ^{181}Ta is under way.

2. Experimental

2.1. Sample preparation and characterization by X-ray-diffraction

High-temperature reaction, frequently in sealed tantalum tubes, and arc-melting of the elements are the routes mentioned in the literature [5–7,9] for the synthesis for transition-metal indium compounds. In the present study we have used arc-melting under argon atmosphere to produce Zr–In samples with a Zr/In ratio of 1:2, 1:3, 2:1 and 3:1. To ensure homogeneity, the molten ingots were turned over, remelted several times and – encapsulated under vacuum in silica tubes – subsequently annealed, usually at 1200 K for 24 h.

To dope the Zr–In compounds with ^{111}In, the mother isotope of the PAC probe ^{111}Cd, two different procedures were tested: (i) ^{111}In-doped In metal was used for the arc-melting. Commercially available, carrier free $^{111}InCl_3$ was deposited onto a thin In foil which was then heated in an H_2 flux for about 1 h to 700 K. The room temperature PAC spectrum of the In foil measured after this procedure corresponded to the well known PAC pattern of ^{111}Cd in metallic In, with the quadrupole frequency $\nu_q(295\,K) = 17.5(2)$ MHz in agreement with the value given in the literature [14]. (ii) In the second procedure ^{111}In was diffused into the molten Zr–In ingots by heating them – together with $^{111}InCl_3$ – for 24 h to 1200 K.

Prior to doping, the compounds were characterized by X-ray diffraction (XRD) measurements, both as-molten and after annealing. It was found that in the as-molten state the compounds were usually not obtained as single-phase materials. In the following we therefore use the notation Zr_x/In_y to differentiate a multiphase sample with Zr/In-ratio x/y from a single-phase compound Zr_xIn_y.

Fig. 1 shows the X-ray diffraction pattern – taken with Cu Kα radiation at room temperature – of a Zr_1/In_2 ingot as-molten (middle section in Fig. 1) and after annealing for 24 h at 1200 K. Comparing the XRD spectrum of as-molten Zr_1/In_2 to that of In metal (bottom-most section in Fig. 1) one finds that – although the sample was remelted several times – most of its strong X-ray reflections originate from In metal. Only a few weak, broad lines (red in the middle section of Fig. 1) belong to the intermetallic phase $ZrIn_2$. By annealing at 1200 K, the X-ray pattern (top-most in Fig. 1) changes to that of an $HfGa_2$-type compound (space group I 41/*a m d* (1 4 1)), reflecting a Zr–In solid state reaction leading to the phase $ZrIn_2$. The room temperature lattice parameters $a = 0.4381$ nm, $c = 2.722$ nm derived from Fig. 1 are in very good agreement with the values reported in the literature [2,6] for $ZrIn_2$.

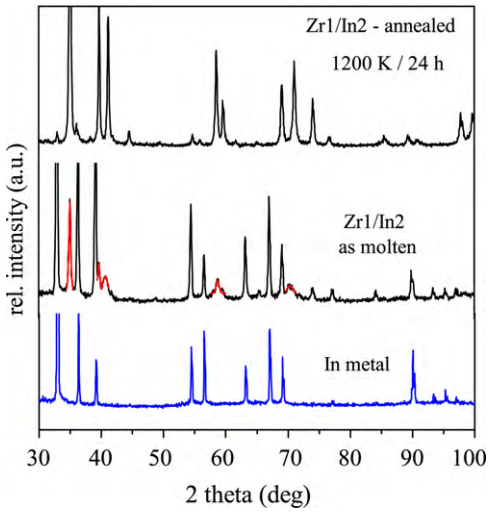

Fig. 1. XRD diffraction spectra (from bottom to top) of In metal, of a Zr_1/In_2 compound in the as-molten state, and of Zr_1/In_2 annealed at 1200 K for 24 h. For the as-molten state of Zr_1/In_2, only the red lines can be attributed to the phase $ZrIn_2$. The other lines originate mainly from In metal. All spectra were taken with Cu Kα radiation at room temperature. (For interpretation of the references to color in this figure legend, the reader is referred to the web version of the article.)

X-ray measurements were also performed for samples of Zr_1/In_3, Zr_2/In and Zr_3/In. The XRD spectrum of Zr_1/In_3 in the as-molten state was very similar to Zr_1/In_2, showing only broad reflections belonging – with comparable intensities – to In metal and to the intermetallic compound $ZrIn_2$. When the Zr_1/In_3 ingot was annealed at 1200 K, the reflections of In-metal disappeared as in the case of Zr_1/In_2. The remaining narrow lines, however, were those of the phase $ZrIn_2$ and not – as we expected – those of $ZrIn_3$.

In contrast to Zr_1/In_2 and Zr_1/In_3, the XRD pattern of as-molten Zr_2/In and Zr_3/In contained no In-metal reflections. Apart from a few non-identified reflections, only the broadened lines of the Au–Cu and Au_3Cu-structure, respectively, were observed. In these cases annealing at 1200 K reduced the line widths, but left the spectra otherwise unchanged. The lattice parameters derived from these spectra are $a = 0.444$ nm, $c = 0.453$ nm for AuCu-type Zr_2In and $a = 0.4457$ nm for Au_3Cu-type Zr_3In, in agreement with the values previously reported in the literature [3,7].

2.2. PAC equipment and data analysis

The PAC spectra were recorded with a standard 4-detector set-up equipped with fast BaF_2 scintillators. Temperatures were varied between 290 K and 1200 K with a PAC furnace described in Ref. [10], for temperatures $15\,K \leq T < 290$ K we used a closed-cycle He refrigerator. Figs. 2 and 3 show as examples the ^{111}Cd PAC spectra observed in Zr_1/In_2- and Zr_1/In_3-ingots, respectively, at different temperatures.

For polycrystalline samples the modulation of an angular correlation by hyperfine interactions can be described by a perturbation factor $G_{kk}(t)$ which depends on the multipole order, the symmetry and time dependence of the interaction, and on the spin of the intermediate state (for details see, e.g., Frauenfelder and Steffen [15]). For a pure static electric quadrupole interaction between the nuclear quadrupole moment Q and an electric field gradient (EFG) at the nuclear site, $G_{kk}(t)$ depends – apart from the nuclear spin I – on 2 parameters: the quadrupole frequency $\nu_q = eQV_{zz}/h$ and the asymmetry parameter $\eta = (V_{xx} - V_{yy})/V_{zz}$ where $V_{ii} = d^2V/di^2$ ($i = x, y, z$) are the principal-axes components of the EFG tensor. When several fractions of nuclei subject to different hyperfine interactions are found in the same sample, the effective perturbation factor is given by:

$$G_{kk}(t) = \sum_i f_i G^i_{kk}(t) \quad (1)$$

Here f_i with $\sum_i f_1 = 1$ is the relative intensity of the ith fraction.

2.3. PAC measurements

2.3.1. Zr_1/In_2 compounds

Fig. 2 shows ^{111}Cd PAC spectra of Zr_1/In_2 samples for the two doping procedures described in Section 2.1. Sample I (SI) was prepared by diffusing ^{111}In into the Zr–In ingot, sample II (SII) was produced by melting Zr metal with ^{111}In-doped In metal.

In the as-prepared state of SI (top-most spectrum in the left-hand column of Fig. 2) the time dependence of the anisotropy with a spin precession period of ~380 ns is characteristic for a perturbation by an axially symmetric QI. A least-squares fit analysis leads to a quadrupole frequency of $\nu_q(295\,K) = 17.4(2)$ MHz. The slow decay of the base-line suggests that a small fraction of the probe nuclei (≤10%) is subject to a broad distribution of much weaker QI's.

Measurements of SI at temperatures $15 \leq T \leq 295$ K revealed a pronounced increase of the dominant QI with decreasing temperature from $\nu_q = 17.4(2)$ MHz at 295 K to $\nu_q = 24.7(1)$ MHz at 15 K (see middle section, left-hand column). This temperature dependence of the QI is identical to the one reported [14] for ^{111}Cd in In metal. It may therefore be concluded that – although SI was produced by arc-melting of the metallic constituents and subsequent ^{111}In diffusion at 1200 K/24 h – the dominant fraction of ^{111}In/^{111}Cd probes of sample I resides on substitutional sites of In metal.

After melting sample I two more times, fast oscillations appeared in the spectrum (middle section, left-hand column) at the expense of the In-metal fraction. A similar pattern – superposition of an In-metal fraction of about 50% and fast oscillations – was found with sample SII (melting of Zr with ^{111}In:In metal) already in the as-prepared state (bottom section, left-hand column).

The right-hand column of Fig. 2 illustrates the changes in the PAC spectra when the samples are heated from 290 K to 1100 K and cooled back to 15 K. The samples were kept for several hours at each temperature. The data shown in Fig. 2 refer to SII, the same trend was observed with SI. At $T \sim 450$ K, near the melting point of In metal, the oscillatory In-metal component gave irreversibly way to four components with different sharply defined QI parameters. For ^{111}Cd in liquid In metal one expects an unperturbed correlation [16]. The absence of a sizeable time-independent component in the PAC spectra therefore indicates that at $T > 450$ K the In metal is consumed in a solid state reaction leading to Zr–In phases.

The relative intensities f, the quadrupole frequency ν_q and the asymmetry parameter η of these components, determined by a least-squares fit analysis based on Eq. (1) are listed in Table 1 for $T = 500$ K. The QI of two of these components (I, II) is axially asymmetric, of the other two (III, IV) axially symmetric. At $T > 800$ K, two components are sufficient to describe the experimental data. As shown in Table 1 for $T = 1100$ K, the axially symmetric components (III, IV) have disappeared. Upon

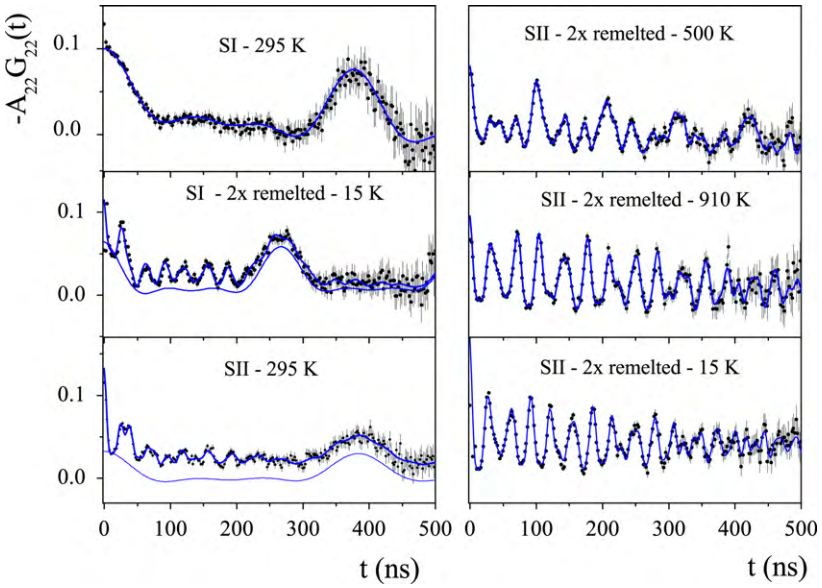

Fig. 2. PAC spectra of ^{111}Cd in two different Zr_1/In_2 samples. Sample I (SI) was synthesized by diffusing ^{111}In at 1200 K/24 h into the intermetallic compound produced by arc-melting of the elements Zr and In. For sample II (SII), In metal was first doped with ^{111}In by diffusion at 700 K/4 h in an H_2 atmosphere and then melted with Zr metal in an arc-furnace.

cooling from 1100 K, these components do not recur, only components I, II persist with constant intensities.

The variation of the QI parameters ν_q, η of components I, II with temperature is shown in Fig. 4. While the asymmetry of component I η(I) is practically temperature independent, η(II) decreases slightly with linear slope $d \ln \eta/dT \sim -1.0(2)\,10^{-4}\,K^{-1}$. The slope of the linear decrease of frequencies ν_q(I) and ν_q(II) with temperature is of the same order of magnitude.

2.3.2. Zr_1/In_3 compounds

The evolution of the ^{111}Cd PAC spectra of Zr_1/In_3-ingots with temperature is illustrated in Fig. 3 for a sample prepared by arc-melting of Zr metal with ^{111}In-doped In metal. Samples prepared by ^{111}In doping of the molten ingot showed a comparable behavior. The left-hand column of Fig. 3 shows the experimental spectra, the right-hand column their decomposition into different components (shifted relative to each other for clarity) by a least-squares fit analysis based on Eq. (1). As in the

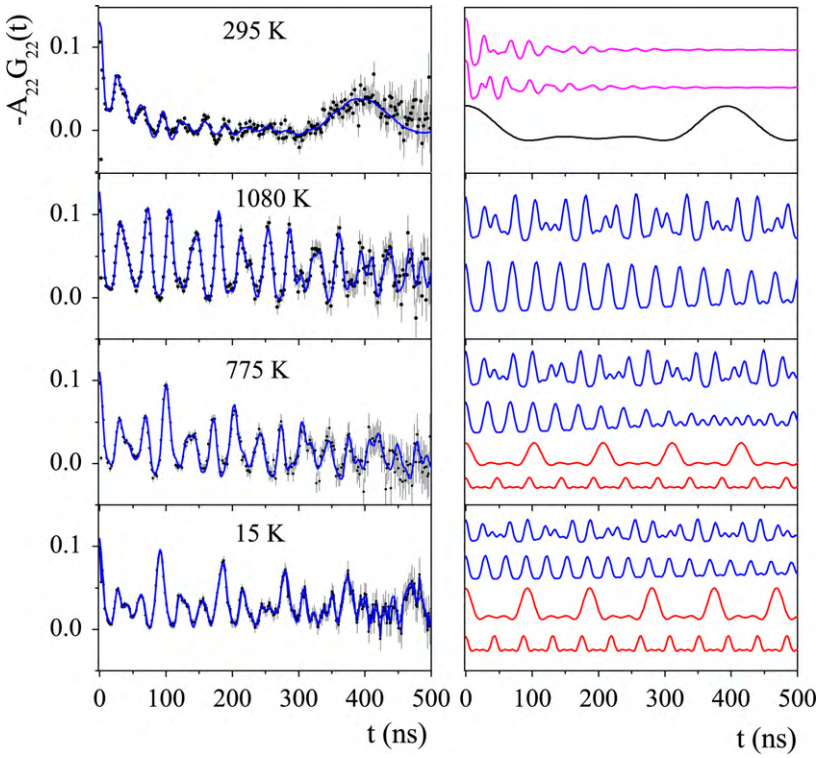

Fig. 3. PAC spectra of ^{111}Cd in a Zr–In ingot produced by arc-melting Zr metal with ^{111}In-doped In metal in the Zr/In ratio 1/3. The assembly of the spectra from top to bottom corresponds to the sequence of measurements: after melting, the compound was taken to 1080 K and subsequently cooled down. Up to four components with different QI parameters are required to describe the experimental spectra at different temperatures (left-hand column). These components are displayed in the right-hand column, shifted relative to each other for the sake of clarity. The comparison of the QI parameters (see Fig. 4) indicates that the blue components are identical to those characteristic for the phase $ZrIn_2$. The red components are assigned to the phase $ZrIn_3$. (For interpretation of the references to color in this figure legend, the reader is referred to the web version of the article.)

Table 1
The relative intensities f and QI parameters ν_q, η of the different components in the ^{111}Cd PAC spectra of a Zr_1/In_2-ingot at 500 K and 1100 K, respectively, observed when the sample was heated from the as-prepared state to 1100 K.

Component	T = 500 K			T = 1100 K		
	Relative intensity f	ν_q (MHz)	η	Relative intensity f	ν_q (MHz)	η
I	0.14_1	110_1	0.98_2	0.34_2	102_1	0.98_2
II	0.14_1	141_1	0.59_1	0.37_2	134_1	0.57_1
III	0.31_1	64_1	0	–	–	–
IV	0.15_1	137_1	0	–	–	–

Note: Here we only consider components with sharply defined QI parameters. An amorphous component characterized by a broad frequency distribution has been neglected. Therefore $\sum_{i=1}^{4} f_i < 1$

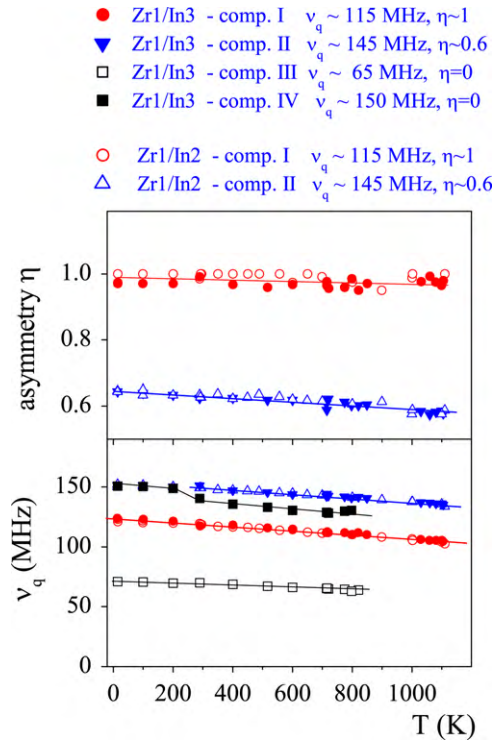

Fig. 4. The quadrupole frequency ν_q and the asymmetry parameter η of ^{111}Cd on the different sites observed in the PAC spectra of Zr_1/In_2 and Zr_1/In_3 samples, respectively, cooled from $T \sim 1100$ K.

case of Zr_1/In_2 (SII and SI remelted), the spectrum of as-molten Zr_1/In_3 (top-most in Fig. 3) consists of an In-metal component with fast oscillations superposed. As for Zr_1/In_2, the In-metal component disappears irreversibly when the compound is slowly heated. As shown by the decomposition in Fig. 3, at $T > 1000$ K the spectrum is well described by two sharply defined components (I, II of Zr_1/In_3). Their intensities f and QI parameters ν_q, η at 1080 K are listed in Table 2. However, upon cooling from 1080 K, two more components (III, IV of Zr_1/In_3) appear in the PAC spectrum at $T \sim 800$ K. This increase in the number of components is reversible, upon heating again to $T > 800$ K only components I, II persist. The QI parameters ν_q, η of these new components III, IV are given in Table 2 for $T = 15$ K. The temperature dependence of ν_q and η of all four components of Zr_1/In_3 is shown in Fig. 4.

In addition to Zr_1/In_2 and Zr_1/In_3, samples of Zr_3/In_1 and Zr_2/In_1 were doped with ^{111}In. Besides the unperturbed component expected for cubic $AuCu_3$-type Zr_3In, the PAC spectrum of Zr_3/In_1 contained a slight In-metal fraction. The case of Zr_2/In_1 requires further studies. Here we observed only a broad QI distribution without any oscillatory components.

3. Results and discussion

The picture projected by XRD for the as-molten ingots is that of poorly crystallized Zr–In phases embedded in a matrix of In metal. When the samples are annealed at 1200 K, the In metal is expended in solid state reactions leading to well crystallized phases such as $ZrIn_2$. As a result, the XRD pattern of non-doped ingots annealed at 1200 K contain – if at all – only traces of non-reacted In metal (see top-most spectrum in Fig. 1).

The heat treatment to which the PAC samples of Zr_1/In_2 and Zr_1/In_3 were exposed during the diffusion process is comparable to the annealing conditions of the XRD samples (1200 K/24 h). It is therefore surprising that in contrast to the absence of sizeable In-metal reflections in the XRD spectra, the room temperature PAC spectra of the as-molten samples are dominated by the In-metal component (see Figs. 2 and 3). At least 50% of the ^{111}In/^{111}Cd probes (concentration $\geq 10^{-8}$ probes/host atoms) reside on substitutional sites of tetragonal In metal. In the case of Zr_1/In_2 doped by diffusing ^{111}In (1200 K/24 h) into the ready ingot (SI in Fig. 1), the In-metal fraction reaches as much as 80%.

This apparent variance of the PAC and the XRD results probably reflects a pronounced preference of the ^{111}In probes for substitutional sites of In metal over In sites in Zr–In intermetallic phases – possibly the consequence of slower diffusion in the intermetallic compound. PAC selectively reflects the local environment of the probe nuclei while XRD averages over the entire sample. Therefore, in case of a marked preference of ^{111}In for In metal sites, the PAC spectrum may still be dominated by the In-metal component, even if the heat treatment has reduced the In-metal concentration of the sample to a level where it escapes XRD detection.

The PAC spectra of Zr_1/In_2 and Zr_1/In_3 contain up to four components I–IV with different QI parameters ν_q, η. Their temperature dependence displayed in Fig. 4 and the values listed in Tables 1 and 2 clearly show that components I, II of Zr_1/In_2 (equal intensities and axially asymmetric EFG; see Table 1) are identical to

Table 2
The relative intensities f and QI parameters ν_q, η of the different components in the ^{111}Cd PAC spectra of a Zr_1/In_3 ingot at 1080 K and 15 K cooled from 1080 K, respectively. In the last column, the components I–IV are assigned to In sites of the intermetallic phases $ZrIn_2$ and β-$ZrIn_3$, respectively. This tentative identification is based on the relative intensities and the symmetry of the QI (see Section 3).

Component	T = 1080 K			T = 15 K			Compound – site (x, y, z)
	Relative intensity f	ν_q (MHz)	η	Relative intensity f	ν_q (MHz)	η	
I	0.42_1	106_1	0.96_1	0.19_2	123_1	0.97_2	$ZrIn_2$-8*e*-In_1 (0, 1/4, 0.28717)
II	0.40_1	137_1	0.59_1	0.21_2	152_1	0.57_1	$ZrIn_2$-8*e*-In_2 (0, 1/4, 0.12556)
III	–	–	–	0.31_1	70_1	0	β-$ZrIn_3$-4*d*
IV	–	–	–	0.15_1	151_1	0	β-$ZrIn_3$-2*b*

those of Zr_1/In_3. In both compounds these components show identical trends $\nu_q(T)$, $\eta(T)$. The same conclusion holds for components III, IV: when present, they have the same intensity ratio 2:1, axial symmetry and identical frequencies in Zr_1/In_2 and Zr_1/In_3.

In Zr_1/In_2 all components I–IV appear during heating, but only I, II persist at $T > 800$ K and subsequent cooling. We therefore associate components I, II with the intermetallic phase $ZrIn_2$ which is consistent with their intensity ratio and QI symmetry. The $HfGa_2$-type structure of $ZrIn_2$ contains two In sites [6]: In_1 (8*e*, coordinates: 0, 1/4, 0.28717) and In_2 (8*e*, coordinates: 0, 1/4, 0.12558). The EFG at both sites is axially asymmetric. A point-charge lattice sum estimate of the EFG contributions of both the Zr and the In sublattice suggests a larger asymmetry for siteIn_1. We therefore tentatively attribute component I to site In_1 and component II to site In_2 of $ZrIn_2$ (see last column of Table 2).

Components III, IV (intensity ratio 2:1, axial symmetry) were observed with identical QI parameters in Zr_1/In_2 during the first heating cycle at $450 \leq T \leq 800$ K and in Zr_1/In_3 (reversibly) at $T \leq 800$ K. We associate these components with the intermetallic phase $ZrIn_3$ which is reported to exist in two modifications: α-$ZrIn_3$ with a $ZrAl_3$-type structure ($D0_{23}$) at low temperature, β-$ZrIn_3$ with a $TiAl_3$-type structure ($D0_{22}$) at higher temperature. The transition temperature between these modifications has not yet been determined.

There are three In sites with axial symmetry (2*a*, 4*e* and 4*d*) in α-$ZrIn_3$ and two In sites, equally of axial symmetry (4*d*, 2*b*), in β-$ZrIn_3$. As the number of In sites and their intensity ratio 2:1 coincides with that of components III, IV (see Tables 1 and 2), we propose to attribute component III to site 4*d*, component IV to site 2*e* of $ZrIn_3$. A definite identification of components I–IV will have to await an electronic structure calculation of the EFG's of the various In sites of $ZrIn_2$, α-$ZrIn_3$ and β-$ZrIn_3$.

On the basis of the proposed correspondence of components I–IV to In sites of the phases $ZrIn_2$ and $ZrIn_3$, the temperature dependence of the relative intensities *f* provides some information on the solid state reactions in the Zr–In system.

In an ingot with Zr:In ratio 1:2, the formation of $ZrIn_2$ passes through the phase $ZrIn_3$. As shown by the data in Table 1, components III, IV (=$ZrIn_3$) are the dominant contributions to the PAC spectrum, when a Zr_1/In_2 ingot is heated for the first time to $T \sim 450$–500 K. Upon further heating, $ZrIn_3$ transforms irreversibly into $ZrIn_2$ (components I, II), as indicated by the disappearance of components III, IV at about 800 K. The Zr–In reactions occurring in a Zr_1/In_2 ingot upon heating may thus be expressed by the sequence: $2Zr + 4In \rightarrow (400\,K) \rightarrow ZrIn_3 + Zr + In \rightarrow (800\,K) \rightarrow 2\,ZrIn_2$.

The solid state reactions taking place in a Zr_1/In_3 ingot are illustrated by the temperature dependence of the relative intensities $f(I) - f(IV)$ in Fig. 5. In this experiment (Section 2.3.2) the Zr_1/In_3 ingot was heated in one step to $T \sim 1100$ K and subsequently cooled to 15 K. At $T \sim 1100$ K, the phase $ZrIn_2$ – rather than β-$ZrIn_3$ – has formed as evidenced by the fact that only components I, II are found in the PAC spectrum. Upon cooling, components III, IV appear at about 800 K, indicating the partial transformation $ZrIn_2 \leftrightarrow$ β-$ZrIn_3$. This transformation is fully reversible. In the temperature range $800 \geq T \geq 400$ K, β-$ZrIn_3$ and $ZrIn_2$ coexist with a ratio $[f(IV) + f(III)]/[f(I) + f(II)] \sim 1/2.5$. At $T \sim 300$ K, another decrease of the $ZrIn_2$ fraction occurs. It is rather improbable that this decrease reflects the emergence of a fraction of α-$ZrIn_3$: there is no evidence of a fifth component in the PAC spectra at $T < 300$ K, as required by a α-$ZrIn_3$ contribution. Instead, the relative intensities $f(III)$ and $f(IV)$, increase without substantial changes in the frequencies of these components. Therefore the decrease of the $ZrIn_2$ fraction more likely mirrors an increase of the β-$ZrIn_3/ZrIn_2$ ratio to ~1/1. For a test of the proposed interpretations a high-temperature XRD investigation of samples of Zr_1/In_2 and Zr_1/In_3 would be of great interest.

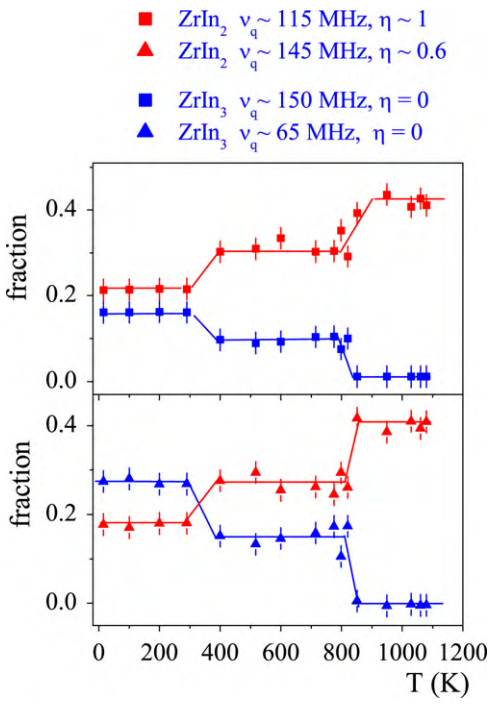

Fig. 5. The relative intensities of the components I, II (red) and III, IV (blue) observed in the ^{111}Cd PAC spectra when an arc-molten Zr_1/In_3 ingot is cooled from 1080 K. Components I, II (red) can be assigned to the phase $ZrIn_2$, components III, IV (blue) to the phase $ZrIn_3$. (For interpretation of the references to color in this figure legend, the reader is referred to the web version of the article.)

4. Summary

We have studied the nuclear electric quadrupole interaction of the nuclear probe ^{111}Cd on In sites in intermetallic compounds of the Zr–In system in the temperature range $15 \leq T \leq 1200$ K by PAC spectroscopy. Compounds with a Zr/In ratio of 1/2 and 1/3 were synthesized by arc-melting of the elemental constituents – usually not as single-phase material – and doped with the probe nuclei by diffusion of ^{111}In at 1200 K. In addition to a large fraction of non-reacted In metal, up to four components with different QI parameters ν_q, η were observed in the PAC spectra. Using their relative intensity and asymmetry parameter, these components have been assigned to In sites of the phases $ZrIn_2$ and β-$ZrIn_3$. Based on this assignment, the temperature dependence of their relative intensities was used to investigate the Zr–In solid state reactions occurring during annealing of arc-molten ingots.

Acknowledgements

M.F. gratefully acknowledges the kind hospitality extended to him at CBPF and the financial support by CNPq. This work has been supported by IPEN/São Paulo by supplying the ^{111}In radioactivity.

References

[1] H. Okamoto, J. Phase Equilib. 11 (1990) 150.
[2] K. Schubert, K. Frank, R. Gohle, A.G. Maldonado, H. Meissner, A. Raman, W. Rossteutscher, Naturwissenschaften 50 (1963) 41.
[3] K. Schubert, H.G. Meissner, A. Raman, W. Rossteutscher, Naturwissenschaften 51 (1964) 287.
[4] A. Raman, K. Schubert, Z. Metallkd. 56 (1965) 44.
[5] S.V. Meschel, O.J. Kleppa, J. Alloys Compd. 333 (2002) 91–98.
[6] M.F. Zumdick, G.A. Landrum, R. Dronskowski, R.-D. Hoffmann, R. Pöttgen, J. Solid State Chem. 150 (2000) 19.
[7] L.D. Gulay, V.I. Zaremba, J. Alloys Compd. 347 (2002) 184–187.
[8] H. Okamoto, Bull. Alloy Phase Diagr. 11 (1990) 412.
[9] R. Pöttgen, R. Dronskowski, Chem. Eur. J. 2 (1996) 800.

[10] M. Forker, W. Herz, U. Hütten, M. Müller, R. Müßeler, J. Schmidberger, D. Simon, A. Weingarten, S.C. Bedi, Nucl. Instrum. Methods A 327 (1993) 456.
[11] M.O. Zacate, A. Favrot, G.S. Collins, Phys. Rev. Lett. 92 (2004) 225901.
[12] M. Forker, P. de la Presa, Phys. Rev. B 76 (2007) 115111.
[13] Wodniecki, A. Kulińska, B. Wodniecka, J. Belošević-Čavor, V. Koteski, J. Alloys Compd. 479 (2009) 56–59.
[14] E. Bodenstedt, U. Ortabasi, W.H. Ellis, Phys. Rev. B 6 (1972) 2909.
[15] H. Frauenfelder, R.M. Steffen, in: K. Karlsson, E. Matthias, K. Siegbahn (Eds.), Perturbed Angular Correlations, North Holland, Amsterdam, 1964, P. 163.
[16] A. Abragam, R.V. Pound, Phys. Rev. 92 (1953) 943.